

Supporting Information for

Pd NP-loaded covalent organic framework for pH-switched Pickering emulsion catalytic dechlorination

Han-Hui Wang[‡], Fei Li[‡], Bing-Jian Yao,^{*} and Yu-Bin Dong^{*}

College of Chemistry, Chemical Engineering and Materials Science, Collaborative Innovation Center of Functionalized Probes for Chemical Imaging in Universities of Shandong, Key Laboratory of Molecular and Nano Probes, Ministry of Education, Shandong Normal University, Jinan 250014, P. R. China.

Email: yaobingjian1986@163.com (B.-J. Yao), yubindong@sdu.edu.cn (Y.-B. Dong)

Content

- 1. Instruments and materials (page S1)**
- 2. Synthesis and characterization of model compound (page S1)**
- 3. Synthesis and characterization of DhaTAPB-COOH (page S3)**
- 4. Synthesis and characterization of Pd@DhaTAPB-COOH (page S10)**
- 5. Preparation and characterization of the Pickering emulsion (page S10)**
- 6. Characterization of model decontamination reaction (page S12)**
- 7. Leaching test and reusable examination (page S14)**
- 8. Scope of decontamination reaction (page S16)**
- 9. References (page S17)**

1. Instruments and materials

All the reagents and chemicals were of analytical grade and were used as received without further purification. $^1\text{H-NMR}$, and $^{13}\text{C-NMR}$ and solid-state ^{13}C CP-MAS NMR spectra were recorded on Bruker Avance-400 HD and AVANCE II 400 spectrometers, respectively. Fourier transform infrared (FT-IR) spectra was conducted on a Bruker ALPHA spectrometer in the $400\text{-}4000\text{ cm}^{-1}$ range. Transmission electron microscopy (TEM) was performed on with an accelerating voltage of 120 kV. Scanning electron microscopy (SEM) was conducted on a Gemini Zeiss SUPRA scanning electron microscope equipped with an energy-dispersive X-ray detector. The X-ray diffraction pattern was measured on a D8 Advance X-ray powder diffractometer with the $\text{Cu } K_{\alpha}$ radiation ($\lambda = 1.5405\text{ \AA}$). Elemental analysis was collected on a Flash EA 1112. X-ray photoelectron spectroscopy (XPS) data was obtained with a PHI 5000 Versaprobe-II electron spectrometer from Ulvac-Phi by analyzing the elements present in the air-facing side of the specimen films with a 90° to the electron beam determined using $300\text{W Al } K_{\alpha}$ radiation. Inductively coupled plasma (ICP) measurement was performed on an IRIS Intrepid (II) XSP and Nu AttoM. Confocal fluorescence microscopy was performed on Leica Microsystems CMS GmbH (TCS SP5 II type) confocal microscopy. The water phase was stained with FITC prior to test. The emulsion was excited by a 488 nm laser. The hydrodynamic size and zeta potential of the samples were measured using a Malvern Zetasizer Nano ZS90 instrument. Water contact angle (WCA) on circular tablet was measured with sessile drop method by a commercial contact angle analyzer (Tracker, France), where a droplet ($2\text{ }\mu\text{L}$) of DI water was deposited on the tablet in air using a precision syringe, the image was captured immediately after droplet deposited on the sample. Profile of the droplet was fitted to the Laplace-Young equation. Gas chromatography (GC) was performed using an Angilent 7890A device.

2. Synthesis and characterization of model compound

A mixture of salicylaldehyde (1.22 g, 10 mmol), aniline (0.93 g, 10 mmol), pyruvic acid ($700\text{ }\mu\text{L}$, 10 mmol), and HOAc (1 mL) in MeCN (20 mL) was reacted for 24 h at $80\text{ }^\circ\text{C}$ under environmental condition. After removal of the solvent in vacuum, the crude product was purified via column chromatography (eluent: dichloromethane) to afford model compound as a yellow solid in 88 % yield.

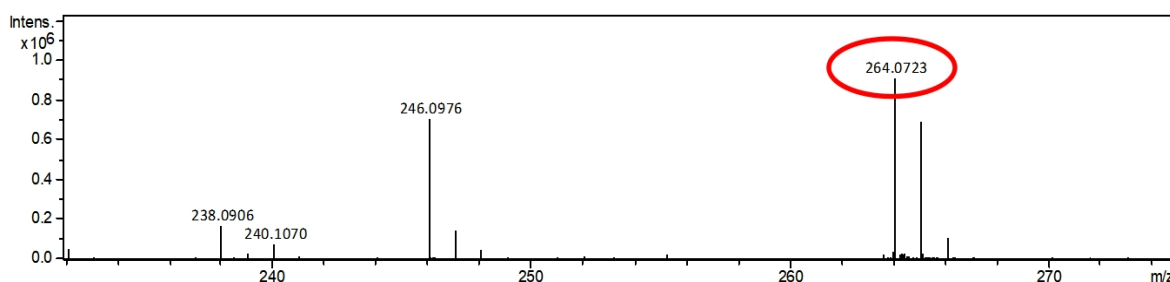


Fig. S1 Mass spectrum of the model compound. ESI-MS m/z calcd for $[\text{C}_{16}\text{H}_{10}\text{NO}_3]^-$ 264.0700, found 264.0723.

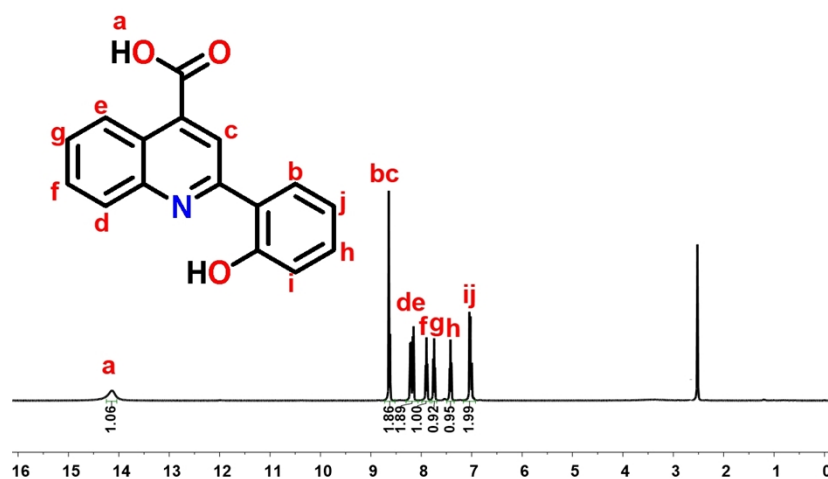


Fig. S2 ^1H NMR spectrum (400 MHz, $\text{DMSO}-d_6$) of the model compound: δ 14.13 (s, 1H), 8.64 (d, 1H), 8.61 (s, 1H), 8.22 (d, 1H), 8.15 (d, 1H), 7.89 (t, 1H), 7.74 (t, 1H), 7.42 (t, 1H), 7.04(d, 1H), 7.01(m,1H).

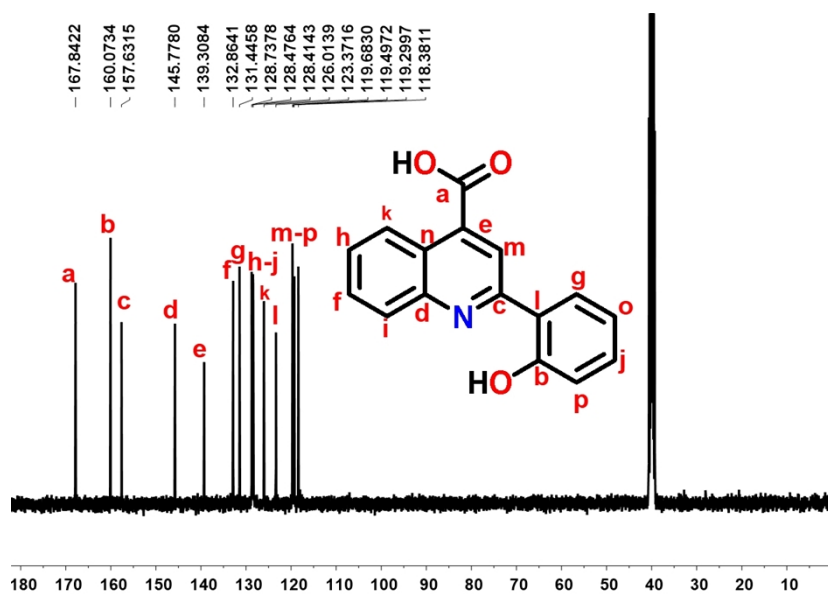


Fig. S3 ^{13}C NMR spectrum (100 MHz, $\text{DMSO}-d_6$) of the model compound: δ 167.8, 160.0, 157.6, 145.7, 139.3, 132.8, 131.4, 128.7, 128.4, 128.4, 126.0, 123.3, 119.6, 119.4, 119.2, 118.3.

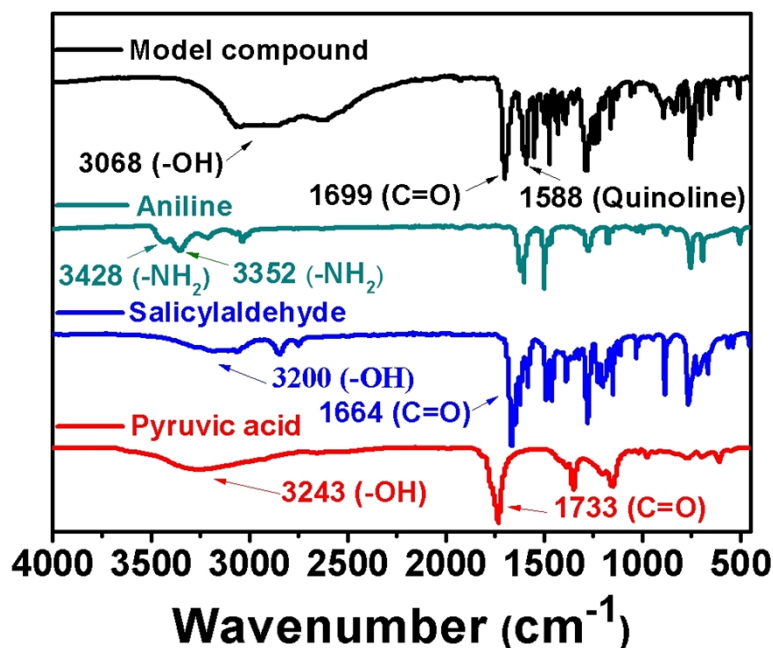


Fig. S4 FTIR spectra (KBr, cm^{-1}) of the model compound and its starting materials: The typical N-H peaks at 3428 and 3352 cm^{-1} in aniline and the C=O peak at 1699 cm^{-1} in salicylaldehyde completely disappeared after reaction. Meanwhile, the new characteristic peaks for C=N at 1588 cm^{-1} demonstrated the formation of the quinolyl moiety in the model compound. The generation of continuous broad peaks around 2600~3068 cm^{-1} indicated an associated state of the model compound due to the presence of hydrogen bond interaction. Additionally, the peak of 1699 cm^{-1} belonging to the carboxylic acid group was also observed.

3. Synthesis and characterization of DhaTAPB-COOH

A mixture of Dha (10 mg, 0.06 mmol), TAPB (14 mg, 0.04 mmol), pyruvic acid (8.5 μL , 0.12 mmol), and HOAc (12M, 0.5 mL) in MeCN (5 mL) was reacted for 7 days at 80 $^{\circ}\text{C}$ under environmental condition. The crude product was completely washing with acetone, THF and ethanol, and then dried under vacuum to afford **DhaTAPB-COOH** as a brick-red crystalline solid in 86 % yield (29.7 mg). FTIR (KBr, cm^{-1}): 1496(-Ar), 1587 (Quinoline), 1719, (-C=O), 2994 (-OH) 3045 (-Ar-H), 3353 (-Ar-OH); Solid-state ^{13}C CP-MAS NMR (400MHz, ppm): 170.7, 153.7, 140.2, 123.3; Anal. Calcd for $(\text{C}_{90}\text{H}_{48}\text{N}_6\text{O}_{18})_n$: C, 72.00; H, 3.22; N, 5.60; found: C, 72.21; H, 3.19; N, 5.58.

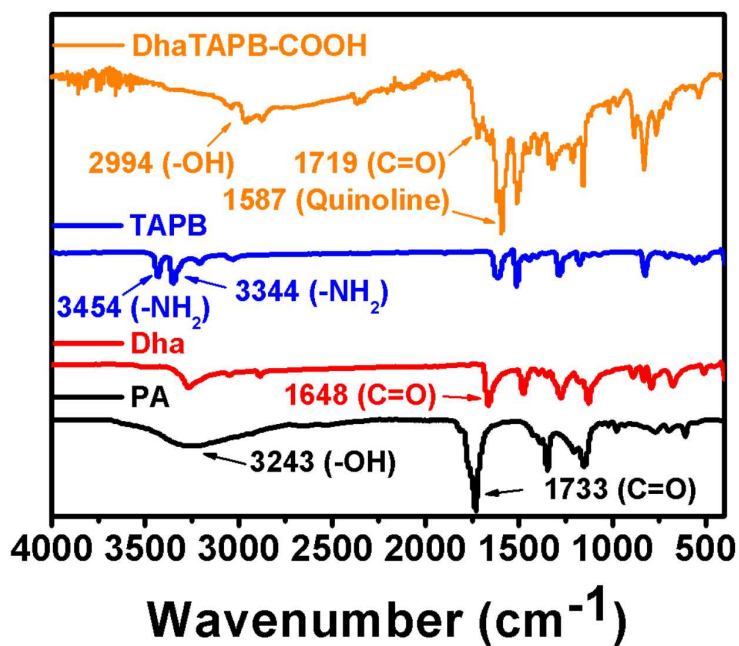


Fig. S5 FTIR spectra of **DhaTAPB-COOH** and its monomers. The typical N–H peaks at 3454 and 3344 cm^{-1} in TAPB and the C=O peak at 1648 cm^{-1} in Dha completely disappeared after polymerization. Meanwhile, the new characteristic peaks for C=N at 1587 cm^{-1} demonstrated the formation of the quinoly moiety in **DhaTAPB-COOH**. Additionally, the peak at 1719 cm^{-1} for the carboxylic acid group was also observed.

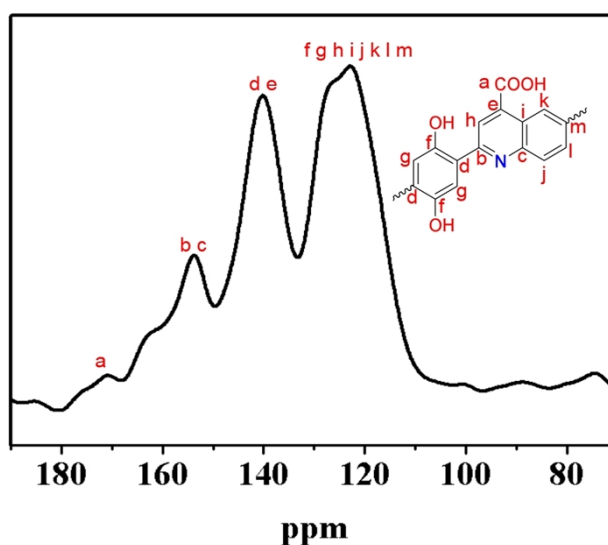


Fig. S6 ^{13}C CP-MAS solid-state NMR spectrum of **DhaTAPB-COOH**. A strong peak corresponding to quinolinecarboxylic acid carbon at 170.7 ppm, a strong peak corresponding to quinoly carbons at 153.7, 140.2, and 123 ppm were clearly observed, indicating the formation of quinoline carboxylic acid linkage. The above assignments were made based on the molecular model compounds and previous literature reports.^{1,2}

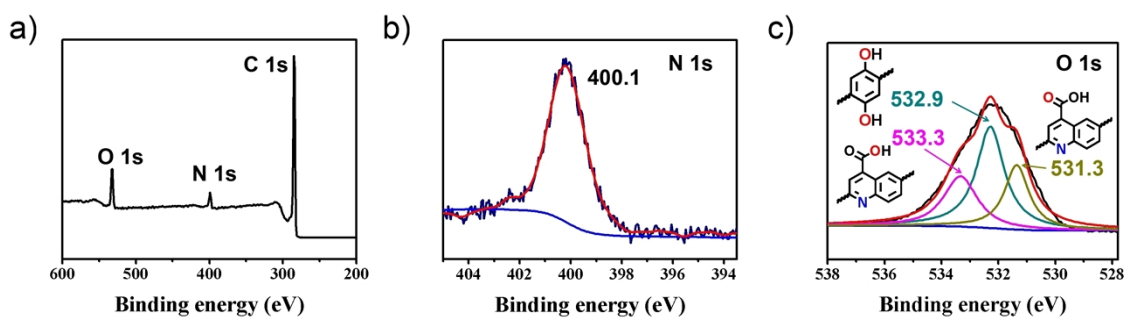


Fig. S7 XPS spectrum of **DhaTAPB-COOH**. The expected elements of C, N, and O appeared in **DhaTAPB-COOH**. The N 1s peak at 400.1 eV and the three forms of O 1s peaks at 533.3 (-COOH), 532.9 (Ar-OH), and 531.3 eV (-COOH) confirmed the formation of quinoline-4-carboxylic acid groups.

Table S1. Fractional atomic coordinates for the unit Cell of **DhaTAPB-COOH**.

DhaTAPB-COOH. AA stacking mode, space group: *P6/m*

$a = 37.2538 \text{ \AA}$, $b = 37.2538 \text{ \AA}$, $c = 3.4794 \text{ \AA}$

$\alpha = 90.0^\circ$, $\beta = 90.0^\circ$, $\gamma = 120.0^\circ$, $R_{wp} = 9.11 \%$ and $R_p = 8.69 \%$

Atom	x	y	z
C1	2.46811	0.63676	0.00023
C2	2.42494	0.61104	0.00024
C3	2.40671	0.56777	0.00024
C4	2.43244	0.55032	0.00022
C5	2.47571	0.57536	0.00021
C6	2.49315	0.61853	0.00022
C7	2.48698	0.6824	0.00023
C8	2.50248	0.5565	0.0002
C9	2.36107	0.54099	0.00025
C10	2.5302	0.708	0.00022
C11	2.54873	0.7513	0.00022
C12	2.52295	0.76909	0.00023
C13	2.4799	0.7438	0.00024
C14	2.46203	0.70076	0.00024
C15	2.33547	0.55861	0.00027
C16	2.29217	0.53385	0.00028
C17	2.27438	0.49027	0.00027
C18	2.29967	0.47252	0.00025
C19	2.34271	0.49769	0.00024
C20	2.48486	0.51328	0.00019
C21	2.50962	0.49474	0.00018
C22	2.5532	0.52053	0.00018
C23	2.57096	0.56357	0.00019
C24	2.54578	0.58144	0.0002
N25	2.53985	0.81089	0.00023
N26	2.23259	0.46538	0.00027

N27	2.57809	0.50362	0.00018
C28	2.56273	0.46195	0.00017
C29	2.59105	0.44459	0.00016
C30	2.57404	0.40143	0.00016
C31	2.59907	0.3834	0.00016
C32	2.64264	0.40867	0.00017
C33	2.65965	0.45183	0.00017
C34	2.63462	0.46987	0.00017
C35	2.67095	0.39131	0.00017
N36	2.65559	0.34964	0.00017
C37	2.68049	0.33273	0.00018
C38	2.66273	0.28969	0.00018
C39	2.68791	0.27182	0.00019
C40	2.73121	0.29677	0.0002
C41	2.74882	0.33998	0.0002
C42	2.72407	0.35852	0.00019
C43	2.75798	0.2779	0.00021
C44	2.74054	0.23473	0.00021
C45	2.76557	0.2165	0.00022
C46	2.80874	0.24222	0.00023
C47	2.82698	0.28549	0.00023
C48	2.80125	0.30294	0.00022
C49	2.87261	0.31227	0.00024
C50	2.74671	0.17086	0.00023
C51	2.70349	0.14526	0.00022
C52	2.68495	0.10196	0.00022
C53	2.71074	0.08417	0.00023
C54	2.75379	0.10946	0.00023
C55	2.77165	0.1525	0.00023
C56	2.89822	0.29465	0.00026
C57	2.94151	0.31941	0.00027
C58	2.9593	0.36299	0.00026
C59	2.93401	0.38074	0.00024
C60	2.89097	0.35557	0.00023
N61	3.0011	0.38788	0.00027
N62	2.69384	0.04237	0.00023
C63	2.58152	0.8372	0.00023
C64	3.02741	0.37252	0.00029
C65	2.65216	0.01606	0.00023
O66	2.65341	0.51217	0.00018
O67	2.58028	0.34109	0.00015
C68	2.20627	0.48074	0.00029
C69	2.1606	0.45242	0.0003

C70	2.59888	0.88288	0.00023
C71	2.64204	0.90902	0.00022
C72	2.66008	0.95209	0.00022
C73	2.6348	0.97038	0.00023
C74	2.59164	0.94424	0.00023
C75	2.57361	0.90117	0.00023
C76	2.13445	0.46944	0.0003
C77	2.09138	0.44441	0.00029
C78	2.07309	0.40084	0.00029
C79	2.09924	0.38382	0.0003
C80	2.1423	0.40885	0.0003
O81	2.5313	0.87765	0.00023
O82	2.16582	0.39007	0.0003
O83	2.06786	0.46319	0.00029
O84	2.70239	0.97561	0.00022
C85	2.49255	0.45122	0.00017
C86	2.51969	0.43547	0.00016
C87	2.26573	0.55093	0.0003
C88	2.22284	0.52379	0.00031
C89	2.59225	0.77774	0.00022
C90	2.60801	0.82064	0.00022
C91	2.74114	0.40204	0.00019
C92	2.714	0.4178	0.00018
C93	2.64144	0.07552	0.00022
C94	2.62568	0.03262	0.00022
C95	2.96796	0.30233	0.00029
C96	3.01085	0.32947	0.0003
C97	0.95286	1.25709	1.00031
O98	0.97869	1.24424	1.00032
O99	0.91438	1.23062	1.00031
C100	1.28083	1.59617	1.00031
O101	1.25499	1.60902	1.00033
O102	1.31931	1.62264	1.00031
C103	1.4473	1.42108	1.00016
O104	1.43446	1.38239	1.00015
O105	1.42084	1.43309	1.00016
C106	1.78638	1.43218	1.0002
O107	1.79923	1.47087	1.0002
O108	1.81285	1.42017	1.0002
C109	1.61129	1.09062	1.00022
O110	1.57261	1.06478	1.00022
O111	1.62331	1.1291	1.00022
C112	1.6224	0.76264	1.00021

O113	1.66108	0.78848	1.0002
O114	1.61038	0.72416	1.0002
H115	2.40402	0.62523	0.00025
H116	2.41824	0.5152	0.00022
H117	2.52827	0.63946	0.00021
H118	2.55101	0.69368	0.00022
H119	2.45924	0.7583	0.00025
H120	2.42687	0.68019	0.00025
H121	2.34979	0.59375	0.00028
H122	2.28517	0.43736	0.00024
H123	2.36328	0.48309	0.00022
H124	2.44973	0.49246	0.00019
H125	2.60611	0.58423	0.0002
H126	2.56038	0.61661	0.00021
H127	2.53896	0.38018	0.00015
H128	2.69473	0.47308	0.00018
H129	2.62758	0.26903	0.00018
H130	2.67331	0.23666	0.00019
H131	2.78396	0.3608	0.00021
H132	2.70542	0.2138	0.00021
H133	2.82967	0.22803	0.00024
H134	2.81544	0.33806	0.00022
H135	2.68268	0.15958	0.00022
H136	2.77444	0.09496	0.00023
H137	2.80682	0.17307	0.00023
H138	2.88389	0.25952	0.00027
H139	2.94851	0.4159	0.00024
H140	2.8704	0.37017	0.00022
H141	2.68338	0.53155	0.12203
H142	2.54861	0.32773	0.122
H143	2.66329	0.8952	0.00022
H144	2.5704	0.95807	0.00023
H145	2.14828	0.50451	0.00029
H146	2.08541	0.34875	0.0003
H147	2.51838	0.89039	0.21269
H148	2.14233	0.34789	0.14622
H149	2.0851	0.4937	0.14621
H150	2.71725	0.96231	0.21267
H151	2.50686	0.40054	0.00015
H152	2.20074	0.53662	0.00032
H153	2.64294	0.84274	0.00021
H154	2.72683	0.45272	0.00018
H155	2.59075	0.01052	0.00022

H156	3.03295	0.31665	0.00032
H157	0.89967	1.18087	1.21053
H158	1.3256	1.64752	1.21053
H159	1.38066	1.40383	1.16794
H160	1.84049	1.44231	1.16799
H161	1.59726	1.13373	1.088
H162	1.64027	0.70671	1.08799

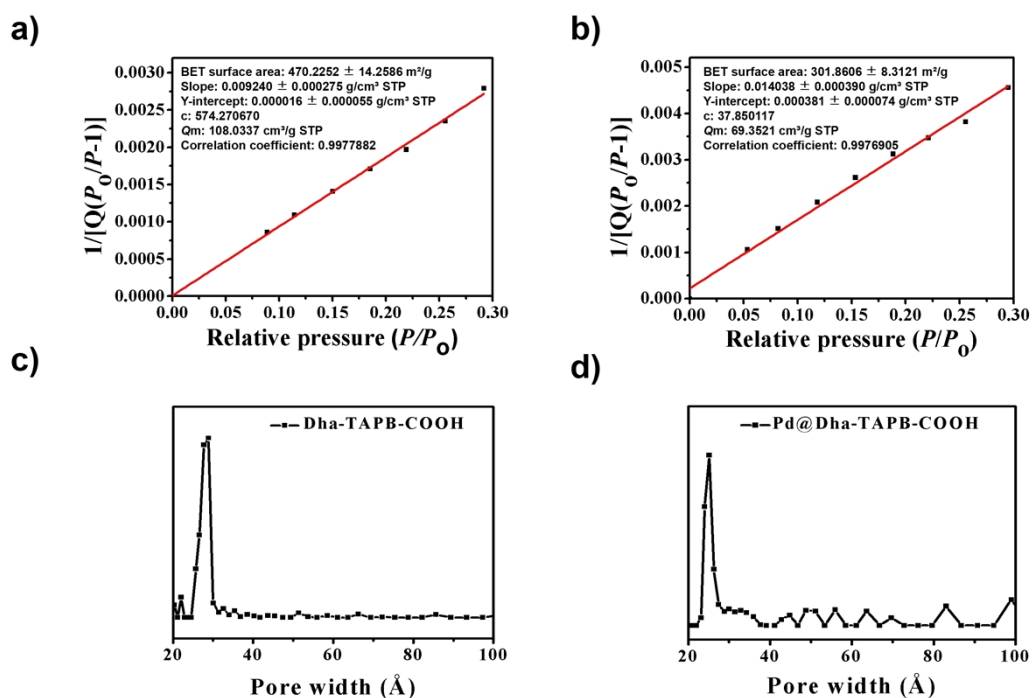


Fig. S8 BET fitting of a) DhaTAPB-COOH and b) Pd@DhaTAPB-COOH carried out using the N_2 isotherm at 77 k. c) Pore size distribution of DhaTAPB-COOH (28.5 \AA) and Pd@DhaTAPB-COOH (23 \AA), respectively.

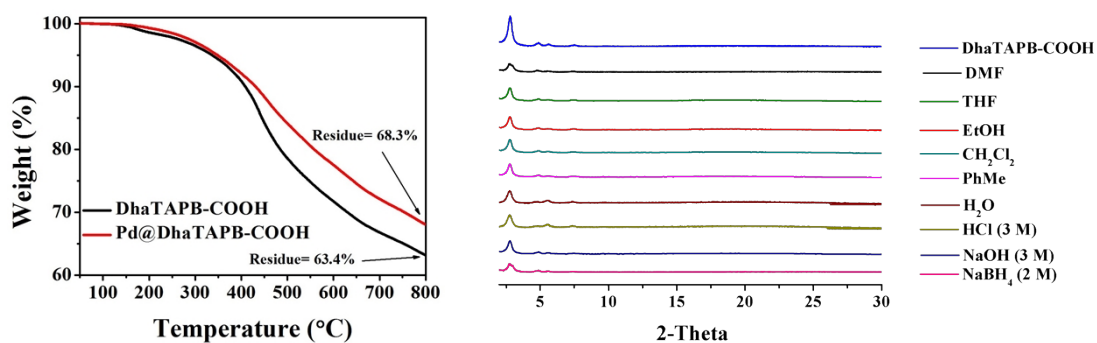


Fig. S9 Left: TGA curves of DhaTAPB-COOH and Pd(II)@DhaTAPB-COOH; Right: PXRD patterns of DhaTAPB-COOH before and after soaking in different media for 24 h.

4. Synthesis and characterization of Pd@DhaTAPB-COOH

DhaTAPB-COOH (100 mg) was added to a MeOH solution (50 mL) of Pd(OAc)₂ (30 mg), and the mixture was stirred at 45 °C for 12 h. The resulting solid was isolated and washed with DCM and dried under vacuum at 60 °C for 6 h. The obtained **Pd(II)@DhaTAPB-COOH** was mixed with NaBH₄ (30 mg) in H₂O (50 mL), and the mixture was stirred at room temperature for 10 h to afford **Pd@DhaTAPB-COOH** as dark brown crystalline solids. The obtained crystalline solids were washed with water, acetone and dried under vacuum at 80 °C for 12 h. As determined by inductively coupled plasma (ICP), the loading amount of Pd NPs was up to 14.1 wt%.



Fig. S10 Photos of **DhaTAPB-COOH** (left) and **Pd@DhaTAPB-COOH** (right).

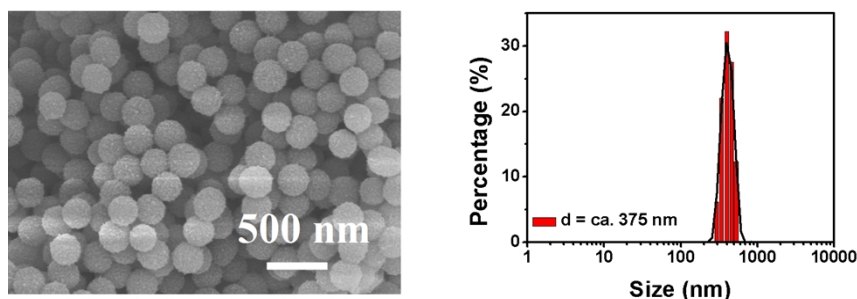


Fig. S11 Left: SEM image. Right: DLS size profile of **Pd@DhaTAPB-COOH**.



Fig. S12 SEM-EDX elemental mapping images of **Pd@DhaTAPB-COOH**.

5. Preparation and characterization of the Pickering emulsion

To prepare the **Pd@DhaTAPB-COOH**-based Pickering emulsion (abbreviated as **Pd@DhaTAPB-COOH-PE**), toluene and deionized water are used as the incompatible oil and water phase, respectively. Typically, **Pd@DhaTAPB-COOH** (55 mg) were added into

a glass vial containing water-toluene (1.2 mL/1.8 mL, 2 : 3 in v/v) mixture. The system was homogenized at 6000 rpm for 60s to generate 2.0 wt% **Pd@DhaTAPB-COOH-PE**. Emulsions with different **Pd@DhaTAPB-COOH** contents and water/oil ratios were fabricated in the similar procedure. Stability of the emulsions was assessed by visual inspection and confocal images before and after long standing. To test the pH-triggered demulsification behaviour of the as-synthesized Pickering emulsions, the pH value was adjusted with 1.5 M HCl and NaOH aqueous solution, respectively. The effect of water-to-toluene ratio, and the content of emulsifiers on the phase separation behavior was investigated by both visual inspection and confocal microscopy.

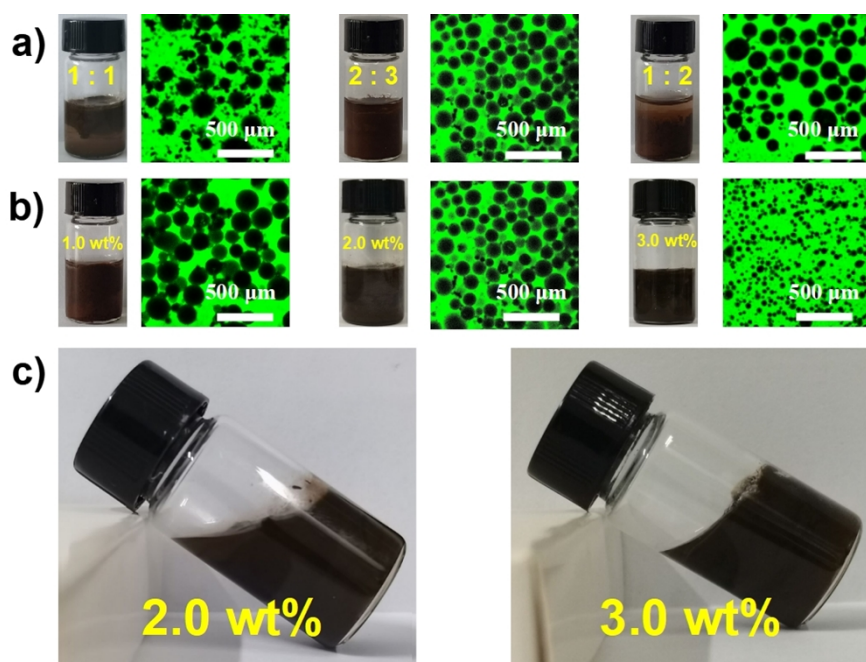


Fig. S13 Visual and confocal microscopy images of **Pd@DhaTAPB-COOH-PE** with different water-to-toluene ratios. b) Corresponding images with different contents of **Pd@DhaTAPB-COOH** (1.0 wt% to 3.0 wt%) in a fixed water-to-toluene ratio of 2 : 3, v/v. For the confocal microscopy images, the aqueous phase was stained with FITC prior to the test, and the emulsion was excited by laser at 488 nm. c) Comparison of the Pickering emulsions stabilized by 2.0 wt% and 3.0 wt% of **Pd@DhaTAPB-COOH**, the latter has a higher viscosity.

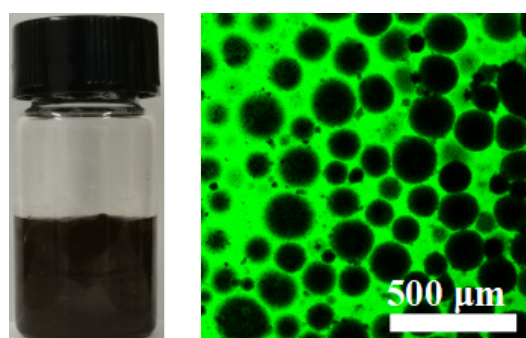


Fig. S14 Visual and confocal microscopy images of **Pd@DhaTAPB-COOH-PE** (2.0 wt%, water-to-toluene ratio of 2 : 3, v/v) after storage naturally for two weeks.

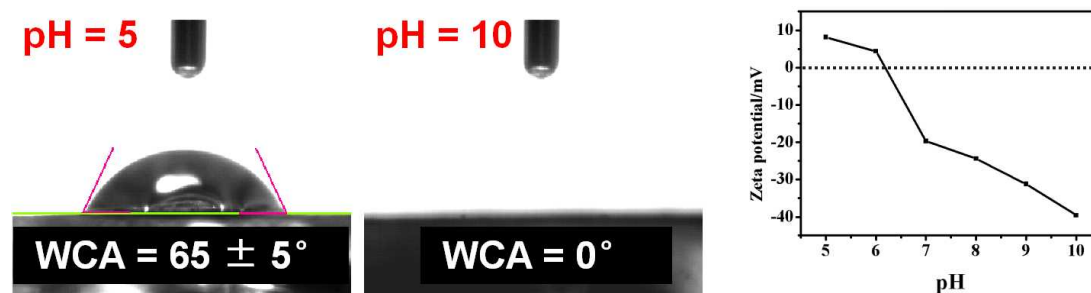


Fig. S15 Water contact angles (WCAs) and zeta potential values of **Pd@DhaTAPB-COOH** measured at different pH values. The WCA value of **Pd@DhaTAPB-COOH** decreased from 65 to 0° when the pH was adjusted from 5.0 to 10.0. Meanwhile, the ζ value gradually decreased from 9 to -40 within the pH range of 5-10, indicating a negatively charged property of **Pd@DhaTAPB-COOH** under alkaline conditions.

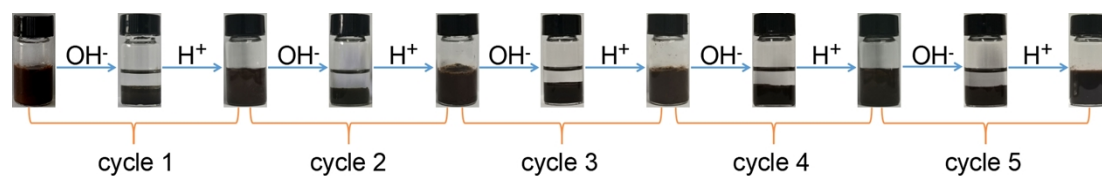


Fig. S16 Visual images of the pH-driven emulsification-demulsification cycles.

6. Characterization of model decontamination reaction

Reaction condition. The biphasic catalytic CBs decontamination reaction was carried over **Pd@DhaTAPB-COOH-PE**. Typically, a mixture of 4-chlorophenol (7.6 mmol) and HCO_2NH_4 (76 mmol) was stirred in the prepared Pickering emulsion with toluene (1.8 mL)-water (1.2 mL) containing 55 mg of **Pd@DhaTAPB-COOH** (2 wt%, 8 mg of Pd NPs, 1.0 mol% equiv). The reaction processed at room temperature in air and it was monitored by GC.

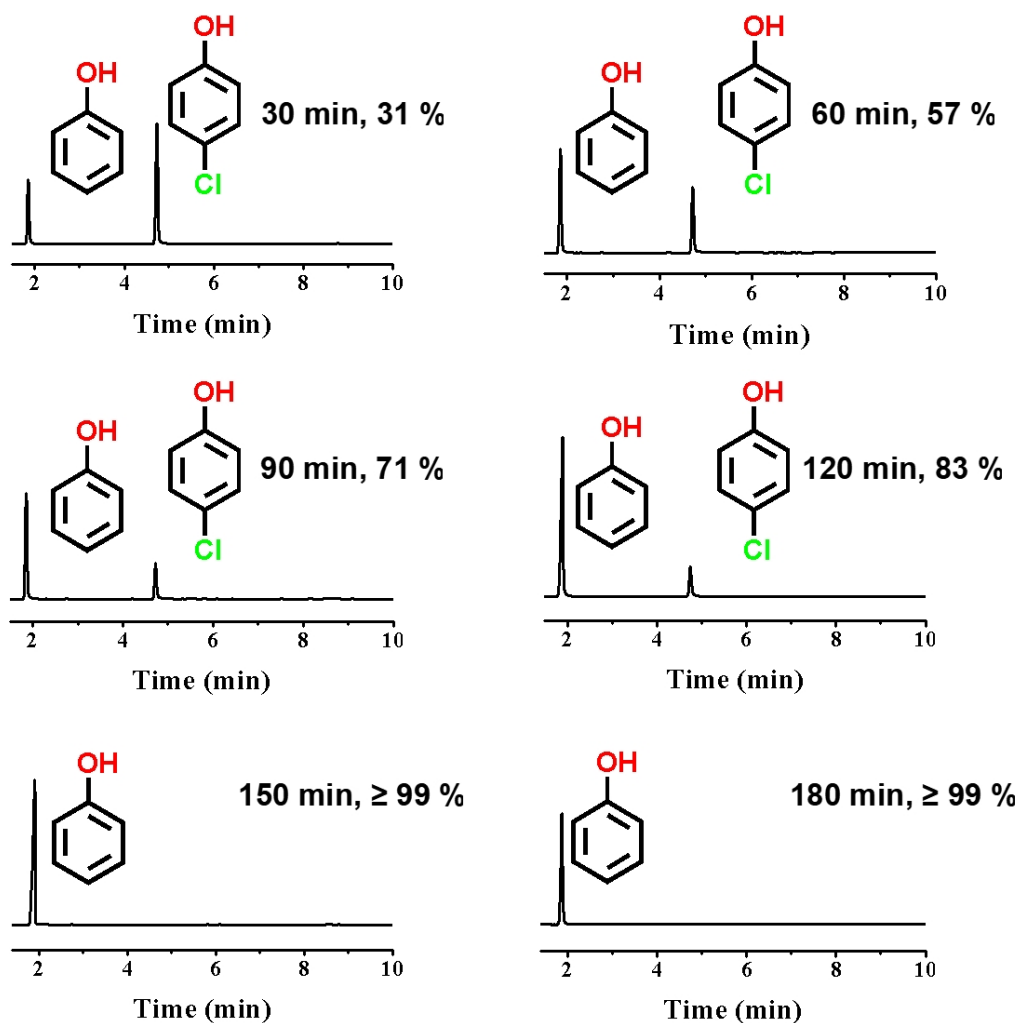


Fig. S17 GC results of the model decontamination reaction at different time intervals.

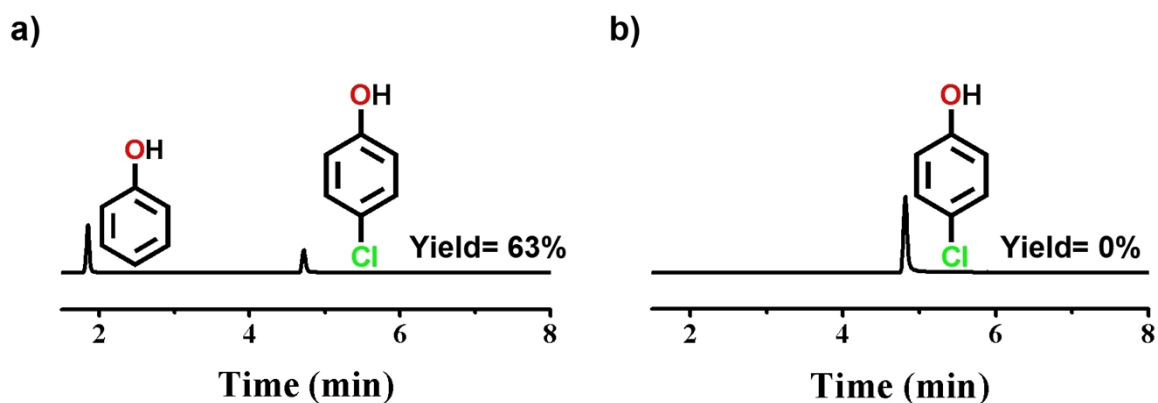


Fig. S18 GC results of a) the model decontamination reaction of the oil-water two-phase mixture system over Pd@DhaTAPB-COOH and b) Pickering emulsion stabilized by 2.0 wt % DhaTAPB-COOH (DhaTAPB-COOH-PE) under given condition, respectively.

7. Leaching test and reusable examination

Catalyst recovery. Once the reaction finished, pH value of the reaction system was adjusted to 10.0 by 1.5 M NaOH aqueous solution with mild stirring. After the complete phase separation, the target organic product in the upper toluene phase was isolated, while the bottom aqueous phase containing **Pd@DhaTAPB-COOH** in the sodium form was collected and reused for the next catalytic run after regeneration via adjusting pH value to ca. 6.0 using aqueous HCl (1.5 M) solution.

Leaching test. The solid **Pd@DhaTAPB-COOH** was separated from the catalytic Pickering emulsion right after reaction for the given time (1.0 h) by centrifugation. The reaction was continued with the filtrate without the aid of **Pd@DhaTAPB-COOH** combining the emulsifier and catalyst. No further increase in the yield of the target product was detected, demonstrating that the active site for the catalytic dechlorination was located on **Pd@DhaTAPB-COOH**.

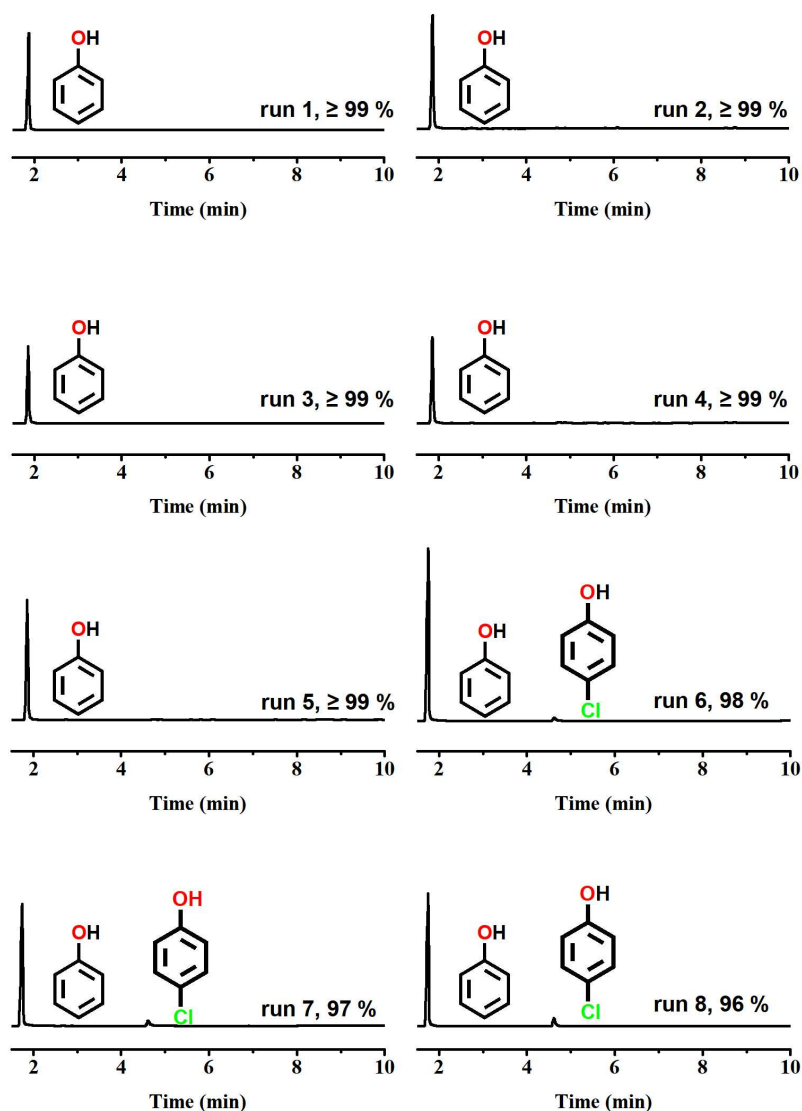


Fig. S19 GC results of the model decontamination reaction for each catalytic run.

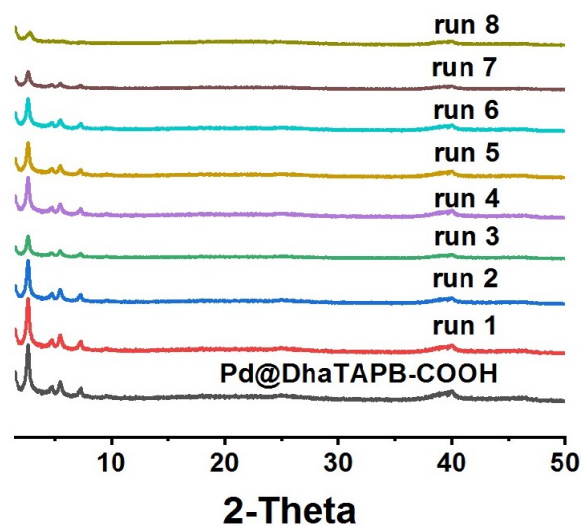


Fig. S20 PXRD patterns of Pd@DhaTAPB-COOH before and after each catalytic run.

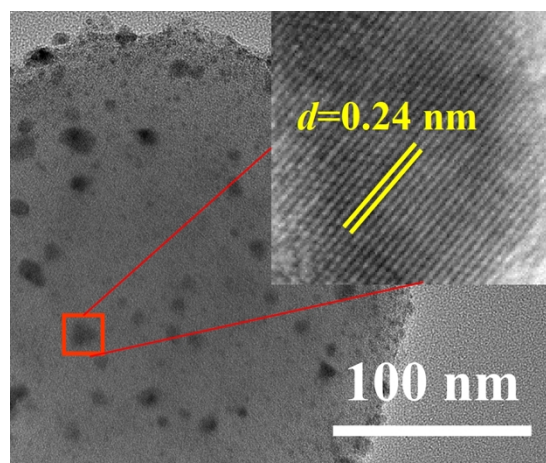


Fig. S21 HRTEM image of Pd@DhaTAPB-COOH after eight catalytic runs.

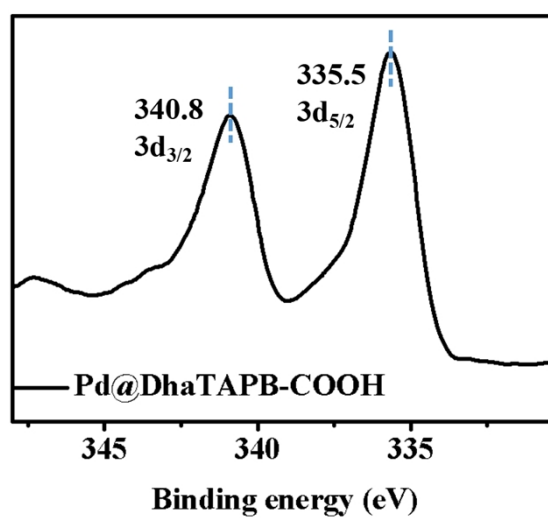
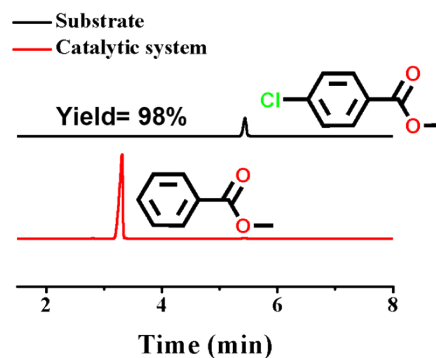
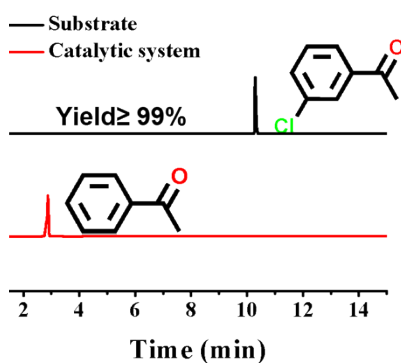
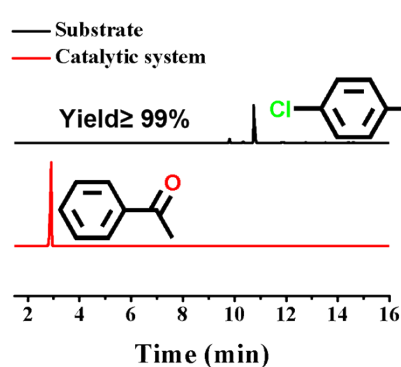
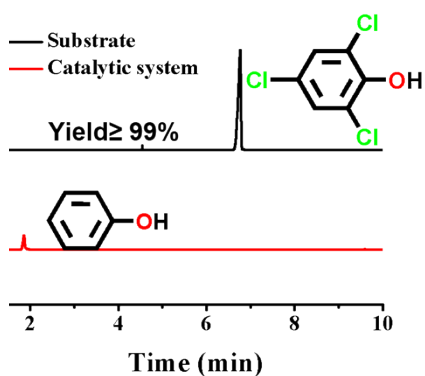
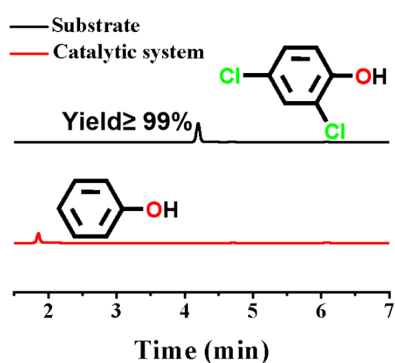
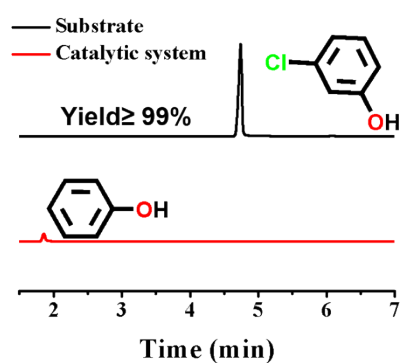


Fig. S22 XPS spectrum of Pd species in Pd@DhaTAPB-COOH after eight catalytic runs.

8. Scope of decontamination reaction

General procedure. The biphasic catalytic CBs decontamination reaction was carried over **Pd@DhaTAPB-COOH-PE**. Typically, a mixture of ArCl (7.6 mmol) and HCO_2NH_4 (76 mmol) was stirred in the prepared Pickering emulsion with toluene (1.8 mL)-water (1.2 mL) containing 55 mg of **Pd@DhaTAPB-COOH** (2 wt %, 8 mg of Pd NPs, 1.0 mol% equiv). The reaction processed at room temperature in air and it was monitored by GC.



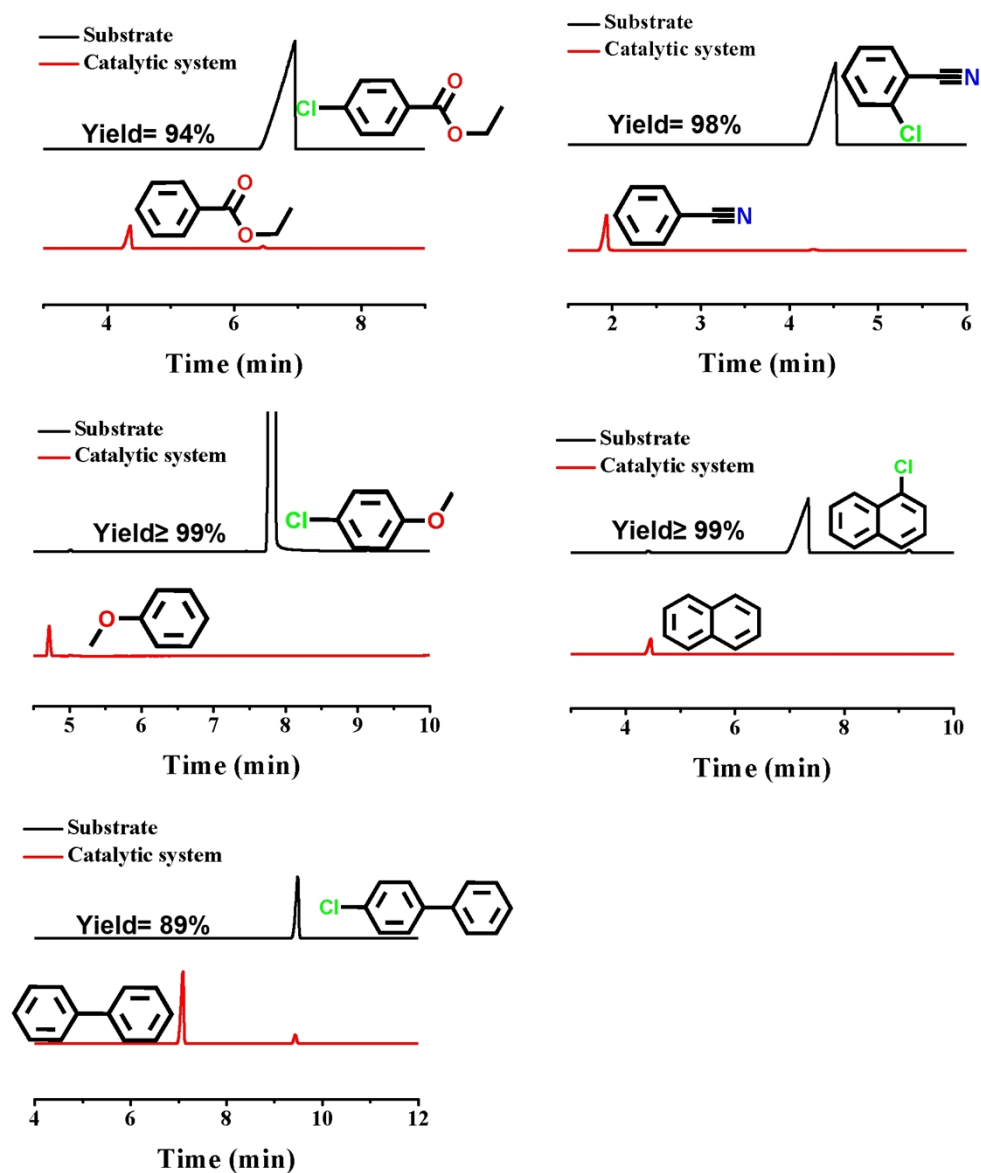


Fig. S23 GC results of the decontamination products generated from different substrates (for Table 1).

9. References

- [1] Y.-L. Yang, L. Yu, T.-C. Chu, H.-Y. Niu, J. Wang and Y.-Q. Cai, *Nat. Commun.*, 2022, **13**, 2615.
- [2] L.-G. Ding, S. Wang, B.-J. Yao, W.-X. Wu, J.-L. Kan, Y.-Y. Liu, J.-Q. Wu and Y.-B. Dong, *J. Mater. Chem. A*, 2022, **10**, 3346–3358